Article

Pyridine N-Alkylation by Lithium, Magnesium, and Zinc Alkyl Reagents: Synthetic, Structural, and Mechanistic Studies on the Bis(imino)pyridine System

Ian J. Blackmore, Vernon C. Gibson, Peter B. Hitchcock, Charles W. Rees, David J. Williams, and Andrew J. P. White

J. Am. Chem. Soc., **2005**, 127 (16), 6012-6020• DOI: 10.1021/ja042657g • Publication Date (Web): 29 March 2005

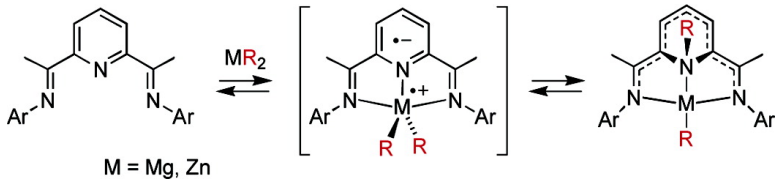

More About This Article

Additional resources and features associated with this article are available within the HTML version:

- Supporting Information
- Links to the 12 articles that cite this article, as of the time of this article download
- Access to high resolution figures
- Links to articles and content related to this article
- Copyright permission to reproduce figures and/or text from this article

View the Full Text HTML

J|A|C|S
ARTICLES
Published on Web 03/29/2005

Pyridine N-Alkylation by Lithium, Magnesium, and Zinc Alkyl Reagents: Synthetic, Structural, and Mechanistic Studies on the Bis(imino)pyridine System

Ian J. Blackmore,[†] Vernon C. Gibson,*[,†] Peter B. Hitchcock,[‡] Charles W. Rees,[†] David J. Williams,[†] and Andrew J. P. White[†]

Contribution from the Department of Chemistry, Imperial College London, Exhibition Road, London SW7 2AY, UK, and Department of Chemistry, University of Sussex, Falmer, Brighton BN1 9QJ, UK

Received December 7, 2004; E-mail: v.gibson@imperial.ac.uk

Abstract: The 2,6-bis(α-iminoalkyl)pyridines 2,6-[ArNC(CR_3)]$_2C_5H_3N$ [R = H, D; Ar = 2,6-*i*-$Pr_2C_6H_3$ (DIPP), 2,6-$Me_2C_6H_3$ (DMP)] react with MeLi in Et_2O to give a binary mixture of products: the pyridine *N*-methylated species 2,6-[ArNC(CR_3)]$_2C_5H_3N$(Me)Li(OEt_2) and the deprotonated/dedeuterated species 2-[ArNC(CR_3)],6-[ArNC(=CR_2)]C_5H_3NLi(OEt_2). For R = D, the product ratio is 2:1 in favor of the N-methylated product, while, for R = H, the deprotonated product is favored by 5:1, increasing to 8:1 in toluene solvent. Warming solutions of the N-methylated species leads to clean conversion to the thermodynamically preferred deprotonated species. Crossover experiments show that MeLi is re-formed and dissociates from the terdentate ligand before deprotonating the ketimine methyl unit. For MgR_2 (R = Et, *i*-Pr) and ZnR_2 (R = Et) reagents, N-alkylation products are formed exclusively, but derivatives containing bulky aryl substituents are found to undergo further rearrangement to 2-alkylated species, arising by migration of the alkyl group of the N-alkyl moiety to the adjacent ring carbon atom. The reversibility of the N-alkylation process has been probed using deuterio-labeled Mg alkyl reagents and mixed alkyl zinc species. A cationic zinc derivative is shown to undergo "reverse" alkyl migration, from the heterocycle nitrogen atom to the zinc center. EPR spectroscopy reveals a paramagnetic intermediate in which the unpaired electron is delocalized over the heterocycle and di-imine moieties of the ligand, indicating that the N-alkylation reactions proceed via single electron-transfer processes.

1. Introduction

Bis(imino)pyridines have attracted considerable interest in recent years due to their capacity to stabilize highly active ethylene polymerization catalysts based on the late transition metals iron and cobalt[1] and the earlier transition metals vanadium[2] and chromium.[3] Despite many investigations directed toward broadening the family of terdentate ligands suited to the stabilization of iron-based catalysts,[4] the productivities have been found to fall off dramatically upon the introduction of significant changes to the bis(imino)pyridine core. There is thus a need to understand why bis(imino)pyridines should be so specially suited to the stabilization of polymerization-active metal centers.

It has long been recognized that conjugated nitrogen ligands, especially imines, can be non-innocent in their coordination chemistry, readily engaging in metal-to-ligand charge transfer and sometimes undergoing alkyl migration reactions. The latter were first extensively documented for α-diimine complexes of magnesium and zinc, where alkylations were observed at the imine carbon and nitrogen moieties, respectively, and shown to proceed via single electron transfer (SET) processes.[5] While the available evidence has suggested that bis(imino)pyridine ligands remain intact during polymerization reactions on iron and cobalt,[1c] it has been found that when attached to vanadium,

[†] Imperial College London.
[‡] University of Sussex.

(1) (a) Small, B. L.; Brookhart, M.; Bennett, A. M. A. *J. Am. Chem. Soc.* **1998**, *120*, 4049. (b) Britovsek, G. J. P.; Gibson, V. C.; Kimberley, B. S.; Maddox, P. J.; McTavish, S. J.; Solan, G. A.; White, A. J. P.; Williams, D. J. *Chem. Commun.* **1998**, 849. (c) Britovsek, G. J. P.; Bruce, M.; Gibson, V. C.; Kimberley, B. S.; Maddox, P. J.; Mastroianni, S.; McTavish, S. J. P.; Redshaw, C.; Solan, G. A.; Strömberg, S.; White, A. J. P.; Williams, D. J. *J. Am. Chem. Soc.* **1999**, *121*, 8728.
(2) Reardon, D.; Conan, F.; Gambarotta, S.; Yap, G.; Wang, Q. *J. Am. Chem. Soc.* **1999**, *121*, 9318.
(3) Estruelas, M. A.; López, A. M.; Méndez, L.; Oliván, M.; Oñate, E. *Organometallics* **2003**, *22*, 395.
(4) (a) Britovsek, G. J. P.; Mastoianni, S.; Solan, G. A.; Baugh, S. P. D.; Redshaw, C.; Gibson, V. C.; White, A. J. P.; Williams, D. J.; Elsegood, M. R. J. *Chem.—Eur. J.* **2000**, *6*, 2221. (b) Ma, Z.; Wang, H.; Qiu, J.; Xu, D.; Hu, Y. *Macromol. Rapid Commun.* **2001**, *22*, 1280. (c) Ma, Z.; Sun, W.-H.; Li, Z.-L.; Shao, C.-X.; Hu, Y.-L.; Li, X.-H. *Polym. Int.* **2002**, *51*, 994. (d) Britovsek, G. J. P.; Gibson, V. C.; Hoarau, O. D.; Spitzmesser, S. K.; White, A. J. P.; Williams, D. J. *Inorg. Chem.* **2003**, *42*, 3454. (e) Chen, Y.; Qian, C.; Sun, J. *Organometallics* **2003**, *22*, 1231. (f) Schmidt, R.; Hammon, U.; Gottfried, S.; Welch, M. B.; Alt, H. G. *J. Appl. Polym. Sci.* **2003**, *88*, 476. (g) Abu-Surrah, A. S.; Lappalainen, K.; Piironen, U.; Lehmus, P.; Repo, T.; Leskelä, M. *J. Organomet. Chem.* **2002**, 55. (h) Chen, Y.; Chen, R.; Qian, C.; Dong, X.; Sun, J. *Organometallics* **2003**, *22*, 4312. (i) Ivanchev, S. S.; Tolstikov, G. A.; Badaev, V. K.; Oleinik, I. I.; Ivancheva, N. I.; Rogozin, D. G.; Oleinki, I. V.; Myakin, S. V. *Kinet. Catal.* **2004**, *45*, 176. (j) Paulino, I. S.; Schuchardt, I. *J. Mol. Catal. A: Chem.* **2004**, *211*, 55. (k) Bluhm, M. E.; Folli, C.; Döring, M. *J. Mol. Catal. A: Chem.* **2004**, *212*, 13. (l) Smit, T. M.; Tomov, A. K.; Gibson, V. C.; White, A. J. P.; Williams, D. J. *Inorg. Chem.* **2004**, *43*, 6511.

10.1021/ja042657g CCC: $30.25

the alkylaluminum cocatalyst can give rise to alkylation at the pyridine carbons of the ligand backbone,[2] presumably via external attack of the cocatalyst on the transition metal bonded bis(imino)pyridine ligand. For chromium[6] and manganese,[7] products arising from ligand coupling reactions are found.

In parallel studies, we[8] and Gambarotta and co-workers[9] found that treatment of bis(imino)pyridines with MeLi unexpectedly afforded a product in which the methyl group had attacked the pyridine nitrogen atom. To our knowledge, this was the first time that nonelectrophilic alkylation at pyridine nitrogen had been documented. In order to understand more about this remarkable reaction and its possible relevance to highly active transition metal polymerization systems, we embarked on a more detailed investigation of the MeLi reaction along with related reactions of bis(imino)pyridines with magnesium dialkyl and zinc dialkyl reagents. Here, we describe synthetic, structural, and mechanistic investigations that examine the site selectivity of the alkylation, the reversibility of the process, the structures of key alkylation products, and the mechanism by which the alkylation process occurs.

2. Results

2.1. Reactivity of Bis(imino)pyridines toward Methyllithium. In a preliminary communication we described the reaction of the partially deuterated 2,6-bis(α-iminoalkyl)-pyridine, 2,6-[(DIPP)NC(CD_3)]$_2C_5H_3N$ ($^2H_6$-**1**, DIPP = 2,6-$Pr^i_2C_6H_3$), with MeLi to give a deep blue solution from which the *N*-methylated product $^2H_6$-**2** was isolated in reasonable (60%) yield.[8] Gambarotta and co-workers found that a closely related, though binuclear, analogue could be isolated using per-protio **1**, and that this compound undergoes a thermal conversion to the de-protonated product **3**.[9] In our hands we had found that the reaction of the per-protio ligand did not afford substantial yields of the *N*-methylated product but rather more of the deprotonated species. The reason for the selective crystallization of the minor product, arising from *N*-methylation, is most probably related to the lower solubility of the dimeric species. We have, therefore, reinvestigated reactions of per-protio and deuterated **1** with MeLi with a view to understanding more about the site selectivity in the protio and deuterio systems.

Treatment of an Et_2O suspension of 2,6-[(DIPP)NC(CD_3)]$_2$-C_5H_3N ($^2H_6$-**1**, DIPP = 2,6-$Pr^i_2C_6H_3$) with 1 equiv of MeLi at −78 °C or at room temperature gave a blue-red dichroic solution. After removal of the volatile components, the ^{1}H NMR spectrum of the crude product revealed a 2:1 mixture of the N-methylated product $^2H_6$-**2** and the dedeuterated product $^2H_5$-**3** (Scheme 1). Selective recrystallization of this mixture from Et_2O gave $^2H_6$-**2** in 50% isolated yield (75% based on $^2H_6$-**2**). Treatment of per-protio bis(imino)pyridine 2,6-[(DIPP)NC-(CH_3)]$_2C_5H_3N$ (**1**) with MeLi under identical conditions also

Scheme 1

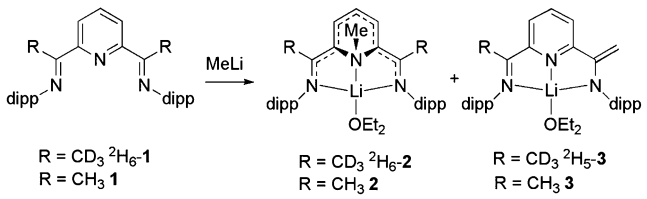

Scheme 2

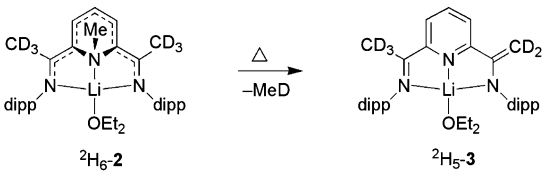

gave a mixture of the N-alkylated product **2** and the deprotonated product **3**, but now in a ratio of 1:5. The greater amount of the deprotonated product compared to the dedeuterated product is consistent with the greater C−D bond strengths associated with the deuterio-methyl derivative. When the reaction was carried out in toluene, different ratios were obtained. For example, $^2H_6$-**1** gave $^2H_6$-**2** and $^2H_5$-**3** in a 1:1 ratio, while ligand **1** gave **2** and **3** in a ratio of 1:8.

Changing the aryl substituents had little effect on the ratio of products. For example, treatment of the 2,6-dimethylphenyl analogue 2,6-[(DMP)NC(CD_3)]$_2C_5H_3N$ ($^2H_6$-**4**, DMP = 2,6-$Me_2C_6H_3$) with 1 equiv of MeLi gave a similar 2:1 mixture of the N-methylated product, $^2H_6$-**5**, and the dedeuterated product, $^2H_5$-**6**.

From the earlier reports, there was an indication that the alkylation reaction is reversible. Gambarotta and co-workers had found that treatment of their binuclear N-methylated complex with *i*PrBr led to the re-formation of **1**,[9] while our studies on reactions of N-methylated $^2H_6$-**2** with $FeCl_3$ had shown that the deuterated bis(imino)pyridine, $^2H_6$-**1**, is regenerated along with a polymerization system (in the presence of added methylaluminoxane, MAO) of comparable activity to (**1**)$FeCl_2$/MAO.[8] In further investigations of the stability of the N-methylated products, complex $^2H_6$-**2** was found to be stable for extended periods at room temperature. However, gentle warming of a C_6D_6 solution to 35 °C or above led to its clean conversion to $^2H_5$-**3** with loss of methane (Scheme 2), a reaction similar to that observed for the per-protio system.

With a view to establishing whether this transformation occurred via an intramolecular pathway, in which the methyl group migrates to the imine carbon with subsequent loss of methane, or via the re-formation of MeLi which dissociates from the ligand and is then available to dedeuterate the ligand backbone, a crossover experiment was performed. A sample of $^2H_6$-**2** was heated in C_6D_6 to 35 °C in the presence of 1 equiv of the per-protio ligand **1** (Scheme 3). The reaction proceeded smoothly and cleanly over 48 h to afford a mixture of $^2H_5$-**3**, **1**, and the crossover products **3** and $^2H_6$-**1**. This provides strong evidence that MeLi is reformed and dissociates from the deuterated ligand prior to deprotonation of **1**.

2.2. Reactivity of Bis(imino)pyridines toward Dialkylmagnesium Reagents. In the case of magnesium alkyls, deprotonation of the ketimine methyl groups does not occur, presumably due to the lower basicity of the magnesium−alkyl moiety

(5) (a) van Koten, G.; Jastrzebski, J. T. B. H.; Vrieze, K. *J. Organomet. Chem.* **1983**, *250*, 49. (b) Kaupp, M.; Stoll, H.; Preuss, H.; Kaim, W.; Stahl, T.; van Koten, G.; Wissing, E.; Smeets, W. J. J.; Spek, A. L. *J. Am. Chem. Soc.* **1991**, *113*, 5606. (c) Kaim, W. *Acc. Chem. Res.* **1985**, *18*, 160. (d) Ashby, E. C. *Acc. Chem. Res.* **1988**, *21*, 414. (e) Wissing, E.; Kaupp, M.; Boersma, J.; Spek, A. L.; van Koten, G. *Organometallics* **1994**, *13*, 2349.
(6) Sugiyama, H.; Aharonian, G.; Gambarotta, S.; Yap, G. P. A.; Budzelaar, P. H. M. *J. Am. Chem. Soc.* **2002**, *124*, 12268.
(7) Reardon, D.; Aharonian, G.; Gambarotta, S.; Yap, G. P. A. *Organometallics* **2002**, *21*, 786.
(8) Clentsmith, G. K. B.; Gibson, V. C.; Hitchcock, P. B.; Kimberley, B. S.; Rees, C. W. *Chem. Commun.* **2002**, 1498.
(9) Khorobkov, I.; Gambarotta, S.; Yap, G. P. A.; Budzelaar, P. H. M. *Organometallics* **2002**, *21*, 3088.

Scheme 3

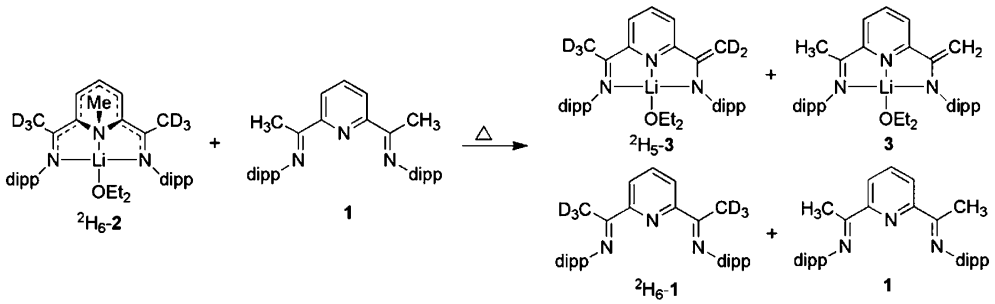

compared to its lithium relative. Therefore, for the study of the magnesium system, per-protio bis(imino)pyridines were employed throughout. Several bis(imino)pyridines reacted cleanly with MgR_2 reagents to give N-alkylated products according to Scheme 4. The relatively unhindered DMP-substituted ligand, **4**, was found to react with $MgMe_2$ to give a deep purple solution indicative of N-methylation. However, workup yielded only an intractable mixture of products. When reacted with $MgEt_2$, **4** gave a similar deep purple solution, but in this case, a clean product, **7**, was isolated. Its ^1H NMR spectrum revealed an AX_2 pattern of resonances centered at 5.55 and 6.73 ppm assignable to the protons at the 4- and 3-positions of the former pyridine ring, respectively, consistent with a mirror plane of symmetry bisecting the central heterocycle. Singlets at 1.82 and 2.21 ppm are attributable to inequivalent methyl substituents of the aryl groups, while a quartet resonance centered at −0.21 ppm is assigned to the methylene unit of the magnesium-bonded ethyl group. A low field quartet resonance at 2.71 ppm is attributable to the methylene protons of the N-ethyl moiety. These data are consistent with the N-ethylated product **7** (Scheme 4). Analogous spectral features were found for the deep red product, **8**, arising from the reaction of **4** with the $MgPr^i_2$ again indicating that alkylation at pyridine nitrogen had occurred.

Scheme 4

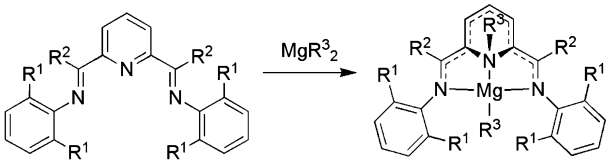

	R^1	R^2
1	Pr^i	Me
4	Me	Me
9	Et	Me
14	Me	H
15	Pr^i	H

	R^1	R^2	R^3
7	Me	Me	Et
8	Me	Me	Pr^i
10	Et	Me	Et
11	Et	Me	Pr^i
12	Pr^i	Me	Me
13	Pr^i	Me	Et
16	Me	H	Pr^i
17	Pr^i	H	Pr^i

In the event that greater steric protection might be required to isolate an N-methylated species, the reaction of the 2,6-diethylphenyl (DEP)-substituted ligand **9** with $MgMe_2$ was investigated. A similar color change to dark purple was observed, but again it did not prove possible to isolate a clean product. However, **9** reacted smoothly with $MgEt_2$ to give the N-alkylated complex **10** and with $MgPr^i_2$ to afford **11** as dark red needles. Over a period of several weeks at room temperature, the latter species slowly underwent a further transformation. We shall return to this shortly (section 2.5).

In a further attempt to isolate an N-methylated species, $MgMe_2$ was reacted with the most sterically hindered bis(imino)-pyridine, **1**. When the reaction was carried out in toluene, a deep blue-purple solid was isolated and found to be the N-methylated species **12**. In diethyl ether, **12** is isolated as a highly crystalline, dioxane-bridged dimer **12a**. The dioxane is carried over from the in-situ-generated $MgMe_2$ and can be removed to afford **12** upon trituration with toluene followed by recrystallization from pentane solution. Upon changing $MgMe_2$ to $MgEt_2$, the N-ethylated product **13** is observed to form by NMR spectroscopy, but it undergoes a rearrangement at a rate comparable with its formation to give a species analogous to that observed upon rearrangement of **11** (see section 2.5).

Treatment of the aldimine ligands **14** and **15** with both $MgMe_2$ and $MgEt_2$ led to intractable mixtures, whereas their reaction with $MgPr^i_2$ led to the isolation of **16** as a bright purple, microcrystalline solid and **17** as a deep red, waxy solid. The isolated yields were relatively low as a result of the high solubility of both products. The absence of backbone methyl groups manifests itself by allowing rapid rotation of the phenyl substituents of **16** on the NMR time scale, a broad singlet resonance now being observed for the *ortho*-methyl substituents.

2.3. Molecular Structures of N-Alkylated Bis(imino)-pyridine Magnesium Complexes. Crystals of **7** and **8** suitable for *X*-ray structure determinations were grown from saturated pentane solutions at room temperature, and crystals of **11** and **12a** were grown from Et_2O solutions at room temperature (Figures 1, 2, 3, and 4, respectively, showing atoms as 50% ellipsoids). Bond parameters for **7**, **8**, **11**, and **12a** are collected in Table 1.

The N-alkylated ligand is very similar in all four structures. When comparing them with complexes of bis(imino)pyridines[1] the most striking feature is the tetrahedral nature of the former pyridine nitrogen where bond angles lie within the range 106°−112° and the bond lengths around this nitrogen are all indicative of single bonds. The bonds through the backbone of the ligand between the imine nitrogens are indicative of delocalization, although the carbon−carbon bonds between the imine functionality and the heterocycle are generally slightly longer. Interestingly, the structures of **7**, **8**, and **11** all show that the N-alkyl group is orientated with the bulky methyl substituents of the ethyl or isopropyl groups directed away from the heterocycle toward the magnesium alkyl fragment. This orientation is favored as it allows the methine or a methylene hydrogen to be directed toward the 4-position of the heterocycle thus

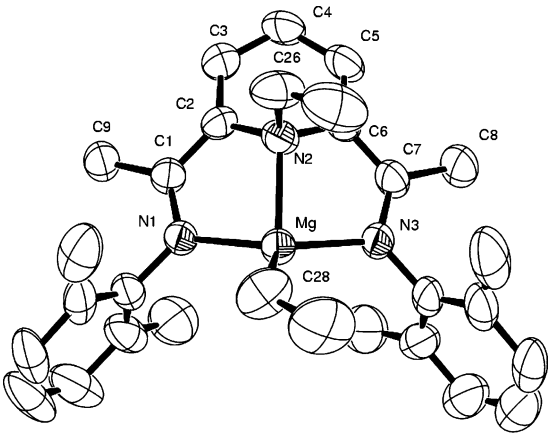

Figure 1. Thermal ellipsoid plot for **7** (at 50% probability level).

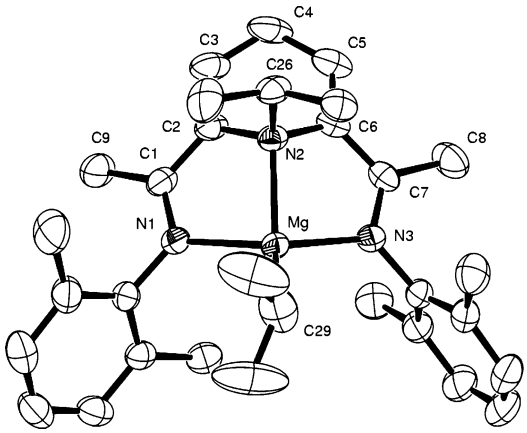

Figure 2. Thermal ellipsoid plot for **8** (at 50% probability level).

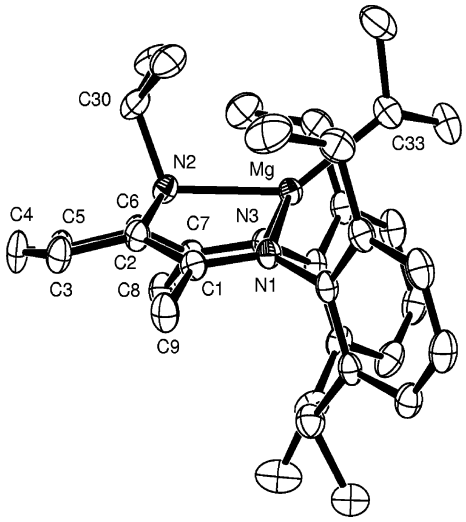

Figure 3. Thermal ellipsoid plot for **11** (at 50% probability level); side view.

minimizing the interaction between the N-alkyl group and the carbons in the 3-, 4-, and 5-positions of the ring which has taken on a "boatlike" conformation. This orientation also has the effect of directing the bulk of the N-alkyl group toward the *ortho*-aryl substituents.

The geometry around the magnesium center in **7**, **8**, and **11** is best described as severely distorted tetrahedral and, in the case of **12a**, as distorted trigonal-bipyramidal with N2−Mg−O as the axial direction. Of perhaps more significance, however,

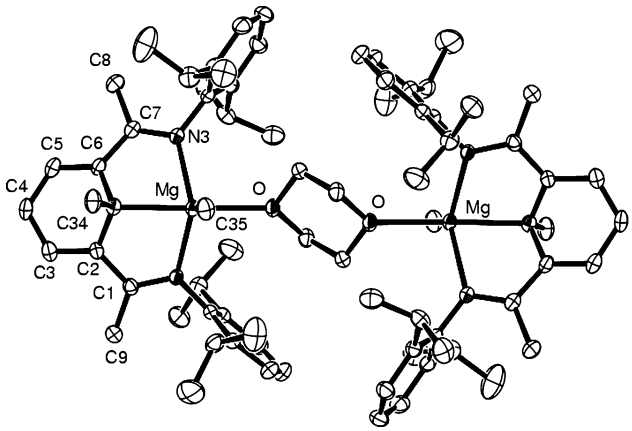

Figure 4. Thermal ellipsoid plot for **12a** (at 50% probability level).

are the bond lengths associated with the magnesium centers, since these become longer as the steric conflict around the magnesium center is increased. The bond lengths in **7** are of less accuracy but are comparable with those in **8**. In the case of **8** the bonds to the imine nitrogens, Mg−N(1) and Mg−N(3), are 2.112(2) and 2.131(2) Å, respectively, and the bond to the heterocycle nitrogen, Mg−N(2), is slightly longer at 2.146(2) Å, while the bond to the isopropyl carbon, Mg−C(29), is 2.122-(2) Å. The magnesium−imine nitrogen bonds in **11** are, on average, slightly longer at 2.147(1) and 2.139(1) Å for Mg−N(1) and Mg−N(3), respectively. The bond to the heterocycle nitrogen, Mg−N(2), is again longer than its counterpart in **8** at 2.180(1) Å as is the magnesium−carbon bond, Mg−C(33), at 2.157(2) Å. The bond lengths associated with the magnesium center in **12a** are again longer, although this may be partially due to the presence of a fifth donor atom, in this case the oxygen of dioxane. The magnesium−imine nitrogen bond, Mg−N(1) and Mg−N(3), are now 2.179(2) and 2.245(2) Å, respectively. The bond to the heterocycle nitrogen, Mg−N(2), is now 2.226-(2) Å, and the bond to the methyl carbon, Mg−C(35), is 2.157-(2) Å. The bond between the magnesium center and the oxygen of the coordinating dioxane is rather long at 2.305(1) Å suggesting a weak interaction.

2.4. Reactivity of Bis(imino)pyridines toward Dialkyl Zinc Reagents. By contrast to $MgMe_2$, treatment of bis(imino)-pyridine ligands with $ZnMe_2$ did not lead to any reaction even after extended periods of time. This is likely to be a consequence of the stronger Zn−C bond strength for Zn−Me relative to its longer chain homologs.[10] Consistently, the reaction between **4** and $ZnEt_2$ proceeded smoothly and cleanly (by NMR) to afford the purple *N*-ethylated complex **18** (Scheme 5) as the sole product after approximately 24 h. Its ^{1}H NMR spectrum revealed a similar series of resonances to those observed for its magnesium analog.

The molecular structure of **18** is shown in Figure 5. It crystallizes with two independent molecules (**A** and **B**, shown in Figure 5a and b, respectively) which have approximately the same conformation. The biggest differences between the two molecules lie in the torsion angles about the N1−Ar bond (ca. 88° and 78° in molecules **A** and **B**, respectively) and in the orientation of the Zn−Et ethyl moiety, the N2−Zn−C28−C29

(10) (a) Bryndza, H. E.; Fong, L. K.; Paciello, R. A.; Tam, W.; Bercaw, J. E. *J. Am. Chem. Soc.* **1987**, *109*, 1444. (b) Britovsek, J. G. P.; Cohen, S. A.; Gibson, V. C.; van Meurs, M. *J. Am. Chem. Soc.* **2004**, *126*, 10701.

Table 1. Selected Bond Lengths (Å) and Angles (deg) for **7**, **8**, **11**, **12a**, and **18** (for **7**, Dimensions Are Given for the Ordered Molecule)

	7 [M = Mg]	**8** [M = Mg]	**11** [M = Mg]	**12a** [M = Mg]	**18** (mol **A**) [M = Zn]	**18** (mol **B**) [M = Zn]
M−N1	2.128(4)	2.112(2)	2.147(1)	2.179(2)	2.115(3)	2.107(3)
M−N2	2.165(4)	2.146(2)	2.180(1)	2.226(2)	2.127(3)	2.133(2)
M−N3	2.131(4)	2.131(2)	2.139(1)	2.245(2)	2.112(3)	2.099(2)
M−C(alkyl)	2.134(6)	2.122(2)	2.157(2)	2.157(2)	1.988(4)	1.981(3)
M−O				2.305(1)		
N2−C2	1.468(6)	1.466(2)	1.470(2)	1.455(2)	1.457(4)	1.458(4)
N2−C6	1.462(6)	1.466(2)	1.468(2)	1.458(2)	1.454(4)	1.453(4)
N2−C(alkyl)	1.506(7)	1.520(2)	1.520(2)	1.495(2)	1.509(4)	1.512(4)
N1−C1	1.317(5)	1.318(2)	1.323(2)	1.326(2)	1.318(4)	1.308(4)
N3−C7	1.320(6)	1.317(2)	1.323(2)	1.324(2)	1.314(4)	1.323(4)
C1−C2	1.409(6)	1.422(2)	1.420(2)	1.412(2)	1.407(5)	1.420(4)
C2−C3	1.389(7)	1.388(2)	1.386(2)	1.392(2)	1.391(5)	1.388(4)
C3−C4	1.392(7)	1.392(3)	1.395(2)	1.388(3)	1.383(6)	1.388(5)
C4−C5	1.383(7)	1.390(3)	1.393(2)	1.396(3)	1.392(5)	1.401(5)
M−N2−C2	110.2(3)	109.1(1)	109.1(1)	111.1(1)	109.8(2)	109.72(18)
M−N2−C6	109.8(3)	109.5(1)	109.0(1)	111.7(1)	110.54(18)	109.66(17)
M−N2−C(alkyl)	107.3(3)	109.4(1)	111.2(1)	106.0(1)	108.55(18)	108.12(18)
C2−N2−C6	107.7(3)	107.1(1)	106.0(1)	109.7(1)	106.8(2)	107.7(2)
C2−N2−C(alkyl)	109.7(4)	112.0(1)	110.0(1)	109.3(1)	109.7(2)	109.7(2)
C6−N2−C(alkyl)	112.2(4)	109.9(1)	111.3(1)	108.9(1)	111.5(3)	112.0(2)
N2−M−O				161.63(5)		
N1−M−O				97.20(5)		
N3−M−O				96.15(5)		
C(alkyl)−M−O				92.85(6)		

Scheme 5

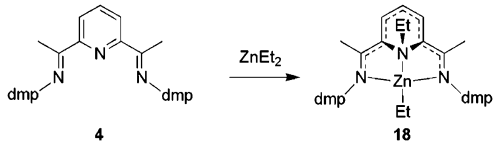

4 **18**

torsion angles being ca. 143° and 160°, respectively. The remaining non-hydrogen atoms for the two independent molecules have an rms deviation for their best fit of ca. 0.07 Å. Interestingly, whereas in the magnesium analogue **7** the N2 and Mg ethyl substituents point to the same side of the molecule (see Figure 1), in both independent molecules of the zinc species **18** the N- and Zn-bound ethyl groups point to opposite sides. The geometry at the metal center in each independent molecule in **18** is distorted tetrahedral with angles in the ranges 79.43(9)°−134.20(15)° in molecule **A** and 79.18(10)°−137.70(12)° in molecule **B**. In each molecule the two most acute angles are associated with the two five-membered *N*,*N*′ chelate rings, and the most obtuse angle is for the N2−Zn−C28 unit. The Zn−R bonds are consistently shorter than their Mg−R counterparts in **7**, and this is most noticeable for the ethyl substituent where the Zn−C bonds [1.988(4) and 1.981(3) Å in molecules **A** and **B**, respectively] are ca. 0.15 Å shorter than the corresponding Mg−C bond in **7** [2.134(6) Å].

2.5. Tautomerization of N-Alkylated Products to C-Alkylated Species. It was found that certain N-alkylated derivatives of zinc and magnesium, especially those bearing more sterically demanding substituents, undergo transformations to give closely analogous products upon standing in solution at room temperature. For example, treatment of a solution of the most sterically hindered bis(imino)pyridine, **1**, with 1 equiv of $ZnEt_2$ initially afforded a dark purple solution indicative of N-alkylation. Monitoring the reaction by ^{1}H NMR spectroscopy (d_2-DCM) revealed the growth of the distinctive AX_2 pattern attributable to the heterocycle protons and a quartet at 2.85 ppm attributable to the N-ethyl group. Also, the growth of a high field quartet at 0.30 ppm attributable to the Zn-ethyl group, a singlet at 1.69 ppm attributable to two equivalent ketimine methyl groups, and a septet at 3.20 ppm attributable to one of the two inequivalent aryl-isopropyl groups are observed. Further characterization of this intermediate was not possible, since it only ever constituted <10% of the reaction mixture and over a period of 10 days it was observed to rearrange to a complex in which the mirror plane of symmetry had been lost. In the ^{1}H NMR spectrum of this second species, resonances were present due to two distinct ketimine methyl groups, along with four septets and eight doublets assignable to four inequivalent isopropyl units. The protons in the 3-, 4-, and 5-positions of the heterocycle are no longer split into an AX_2 pattern but instead give an AMX pattern. Complex multiplets, at 1.74 and 0.48 ppm, are attributable to the methylene protons for two distinct ethyl environments. Significantly, it is the resonance associated with the N-ethyl moiety that has undergone the most significant change in chemical shift. An HMBC NMR experiment revealed coupling between the methylene carbon of the ligand ethyl group and the protons in the 4-position and one of the protons in the 3-position of the heterocycle. The carbon in the 2-position of the heterocyclic ring was confirmed as a quaternary carbon by a DEPT-135 experiment and was observed to couple with the methylene and methyl protons of the ligand ethyl group and the protons in the 3- and 4-positions of the heterocycle. These observations are consistent with the ethyl group being attached to the 2-position of the heterocyclic ring and indicates that migration of the ethyl unit from nitrogen to carbon had occurred (Scheme 6). Attempts to grow crystals of this product suitable for a single-crystal X-ray diffraction study were unsuccessful. For the analogous reaction of **1** with $MgEt_2$, the N-ethylated species **13** is formed initially, but it cannot be isolated, since it rearranges to a product with similar spectral features to its zinc relative and consistent with the 2-alkylated tautomer. When the size of the aryl group is reduced to DEP, the rearrangement is no longer observed unless the size of the

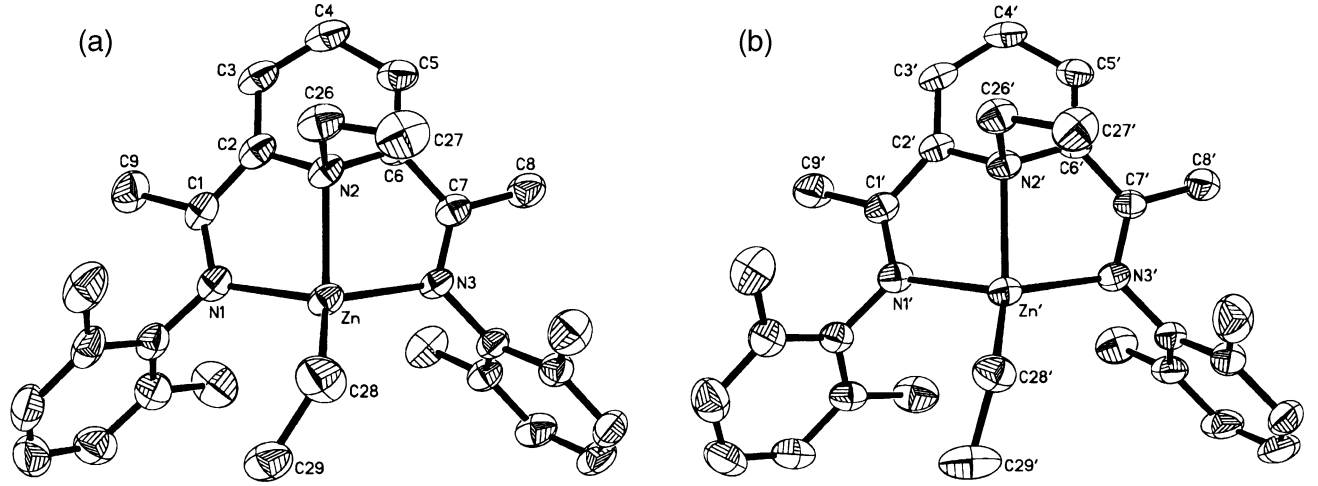

Figure 5. Structure of the two independent molecules present (**A** in part a, **B** in part b) in the crystals of **18** (50% thermal ellipsoids, chemical numbering scheme).

magnesium alkyl is increased to isopropyl, suggesting that the alkyl migration is largely driven by steric factors.

Scheme 6

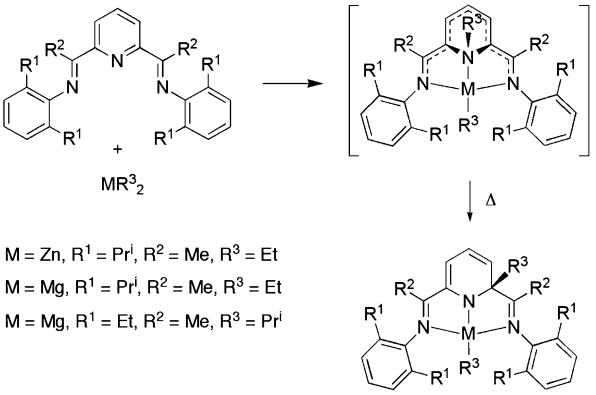

2.6. Reversibility of the N-Alkylation Reactions. The reversibility of the N-alkylation reactions has been probed by deuterium labeling studies. Addition of 1 equiv of $Mg(CD_3)_2$ to a sample of **12** in C_6D_6 led to a decrease in the intensity of the magnesium methyl resonance as it rapidly exchanged with the deutero-methyl groups of $Mg(CD_3)_2$ (Scheme 7). Over a period of approximately 48 h the signal assigned to the N-methyl group also decreased in intensity as it too was replaced by deutero-methyl groups. Although this suggests that the N-alkylation is indeed reversible (a direct exchange between the N-methyl group and $Mg(CH_3)_2$ seems unlikely), it does not inform as to whether in this case the $Mg(CH_3)_2$ first dissociates from the ligand as opposed to the N-methyl group simply migrating back and forth between the magnesium and the pyridine nitrogen until the two sites are equilibrated. The reaction between $Mg(C_2D_5)_2$ and **7** led to similar observations, but in this case, the incorporation of deutero-ethyl groups at the pyridine nitrogen took 6 weeks to reach equilibrium.

To determine whether $MgMe_2$ or $MgEt_2$ first dissociate from the ligand, **12** was monitored in the presence of 1 equiv of $^2H_6$-**1**. This led to the slow evolution of **1** with concomitant formation of $^2H_6$-**12**, the reaction reaching equilibrium after approximately 6 weeks at room temperature (Scheme 8). By contrast, addition of 1 equiv of $^2H_6$-**4** to **7** did not lead to any evolution of **4** or uptake of $^2H_6$-**4** even after 6 weeks, indicating that $MgEt_2$ does not dissociate from the ligand, at least on the time scale of this experiment.

Scheme 7

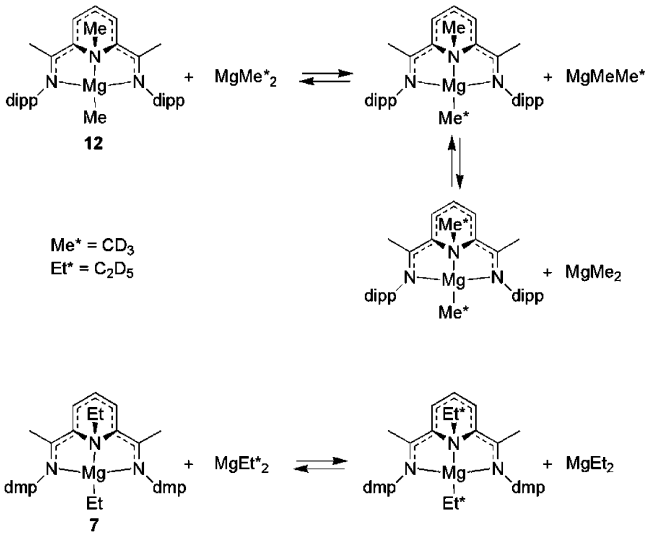

Due to the less ready availability of deutero-alkyl zinc reagents, a modified approach was adopted for the zinc system. In this case, the mixed Et/OPr^i complex **19** was first synthesized by alcoholysis of **18** using Pr^{i}OH in the presence of a catalytic amount of $[H(Et_2O)_2][BAr^f_4]$. **19** was then treated with 1 equiv of $Mg(C_2D_5)_2$ to give the mixed $[ZnEt(C_2D_5)]$ complex, **20** (Scheme 9). If *N*-ethylation is reversible, then "scrambling" of the deutero- and protio-ethyl groups in **20** would occur. Since this was not observed after a period of approximately 6 weeks, it can be concluded that the N-ethylation in this complex is not reversible. Consistently, addition of the deuterated ligand $^2H_6$-**4** to complex **18** afforded no exchange after approximately 6 weeks. Similarly, no scrambling of the ethyl and methyl groups in **21** was observed, though this may be due, in part, to the stronger ZnMe bond.

2.7. Cationic Derivatives. Complex **18** was treated with 1 equiv of the strong Lewis acid $B(C_6F_5)_3$ in order to abstract the zinc ethyl group and to form a cationic complex. Over the course

Scheme 8

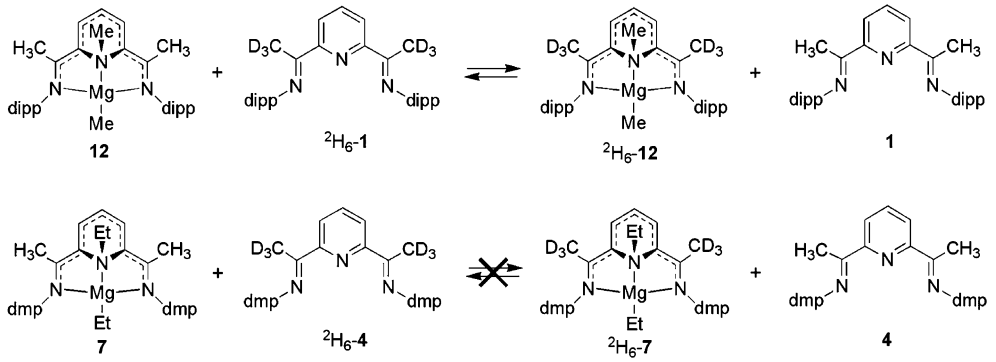

of approximately 24 h **18** was completely consumed and the ^{1}H NMR spectrum revealed a shift of the AX_2 pattern from its position at 5.54 and 6.94 ppm to 8.59 and 8.38 ppm, indicative of aromatization of the pyridine heterocycle. The presence of a $EtB(C_6F_5)_3^-$ counterion is shown in the ^{1}H NMR spectrum by

Scheme 9

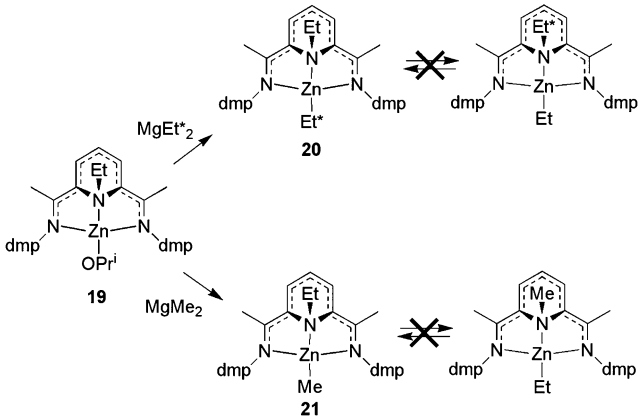

the presence of broad quartet and triplet resonances centered at 1.10 and 0.52 ppm, respectively, whereas a zinc−ethyl group is revealed by the presence of quartet and triplet signals at 0.20 and 0.46 ppm, respectively. The ^{19}F NMR spectrum gave resonances at −134.9 ppm, −167.5 ppm, and −170.1 ppm, consistent with a noncoordinated $EtB(C_6F_5)_4^-$ counterion.[11] These observations indicate that an ethyl group is abstracted to give the cationic ethyl complex **22** presumably via a short-lived cationic N-alkyl intermediate (Scheme 10).

To determine whether it is the N-ethyl that is abstracted, or rather the zinc ethyl followed by migration of the N-ethyl group to the zinc center, the mixed alkyl complex **21** was treated with $B(C_6F_5)_3$ in d_8-THF; THF is used as the NMR solvent here because **21** is generated in situ by using $MgMe_2$ which is incompatible with d_2-DCM. In this case, the zinc methyl resonance underwent a significant downfield shift from −1.15 ppm to 0.5 ppm indicative of formation of the $[MeB(C_6F_5)_3]$ anion.[10] The resonances associated with the N-ethyl group and the AX_2 pattern assigned to the heterocycle protons showed only small shifts. Analogous results were obtained upon treatment of **18** with $B(C_6F_5)_3$ in d_8-THF. These observations allow us to conclude that $B(C_6F_5)_3$ reacts preferentially with the zinc-bonded alkyl group rather than the N-alkyl moiety, but here the N-ethyl

(11) (a) Coles, M. P.; Jordan, R. F. *J. Am. Chem. Soc.* **1997**, *119*, 8125. (b) Yang, X.; Stern, C. L.; Marks, T. J. *J. Am. Chem. Soc.* **1994**, *116*, 10015.

Scheme 10

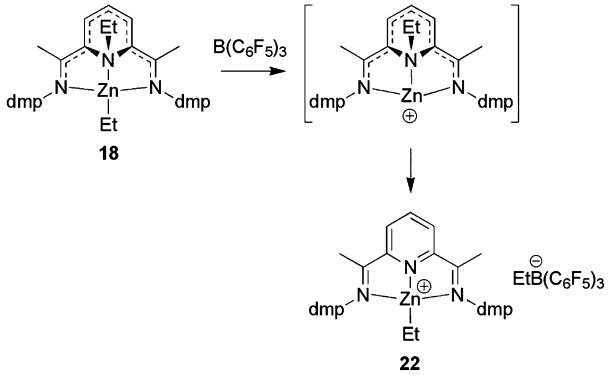

Scheme 11

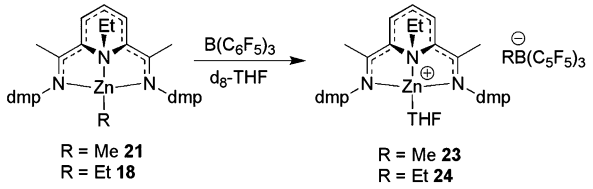

group does not migrate to the zinc center due to strong binding of THF (Scheme 11), indicating that coordinative unsaturation is a prerequisite for migration of the alkyl group back to the metal center.

2.8. Mechanism of Alkylation. The mechanism of alkylation processes at imino carbon and nitrogen centers of α-diimine ligands have been shown to involve single electron-transfer processes, and in many cases, the products of alkyl radical coupling reactions are observed as byproducts.[5] For the reactions described here no products arising from coupling of alkyl radicals are observed by ^{1}H NMR spectroscopy, and despite the diamagnetic nature of all of the complexes, we decided to examine them by EPR spectroscopy in an attempt to identify potential radical intermediates. Complexes $^2H_6$-**2** and **18**, for which the N-alkylation had been shown to be irreversible at room temperature, gave no discernible signal. Complex **7** gave a very weak EPR signal, while for complex **12**, where N-alkylation has been found to be readily reversible, a strong, though rather complex, EPR signal was observed. The spectrum obtained at 175 K is shown in Figure 6 along with a simulated spectrum for a radical delocalized over both the imine and pyridyl moieties. Since the N-alkylated product and the proposed ligand−$MgMe_2$ adduct present in the equilibrium are diamag-

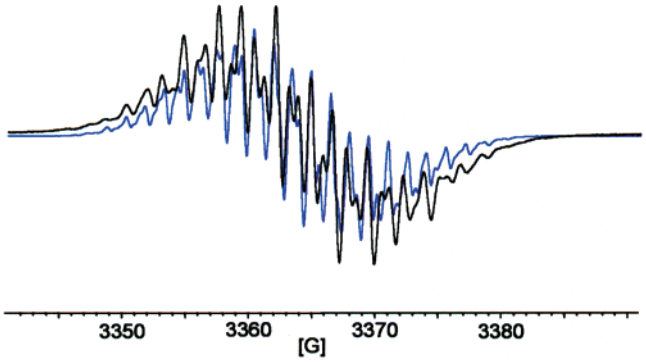

Figure 6. Experimental (black) and simulated (blue) EPR spectra of **12** at 175 K.

netic, the signal is likely to arise from a radical intermediate such as that shown in Scheme 12.

Scheme 12

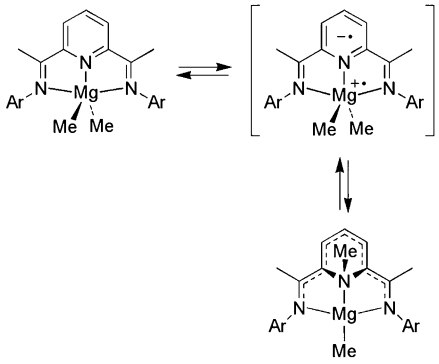

3. Discussion

The differing ratios of N-methylated to deprotonated (and dedeuterated) species in the per-protio and deuterio systems are readily explained by a kinetic isotope effect. The observation that the *N*-methylated species is converted, on warming, to the thermodynamically preferred deprotonated product suggests that the unconventional N-alkylating capacity of MeLi arises from initial complexation of MeLi by the tridentate ligand, followed by migration of the methyl group to the adjacent N-atom. The loss of aromaticity of the pyridine ring is evidently compensated by the extensive delocalization of the negative charge over the heterocyclic ring and the imino groups of the ligand backbone. The crossover experiments confirm that this process is finely balanced energetically, the reverse process readily occurring to liberate MeLi which is then available to deprotonate the ketimine methyl moiety. The observation of both the N-methylated and the dedeuterated products in the low-temperature reaction of MeLi with deuterio-bis(imino)pyridines is reflective of a kinetic product distribution arising from initial attack by MeLi on the ligand backbone (dedeuteration) versus MeLi complexation by the terdentate bis(imino)pyridine prior to alkyl migration.

By contrast to lithium alkyls, magnesium and zinc dialkyl reagents are insufficiently basic to deprotonate/dedeuterate the ketimine units, thus allowing a more detailed study of the factors directly affecting the N-alkylation process, as well as the stability of the N-alkylated products. Table 2 gives a summary of the products arising from treatment of bis(imino)pyridines with a range of magnesium alkyl reagents, revealing a relatively narrow window in which the N-alkylated products are stable.

Table 2. Summary of Reaction Products Arising from Treatment of MgR_2 Reagents with Bis(aldimino)pyridines and Bis(ketimino)pyridines Bearing Differing Aryl Substituents

	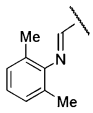	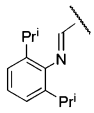	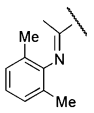	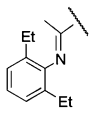	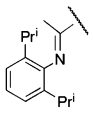
$MgMe_2$	Intract. mixture	Intract. mixture	Intract. mixture	Intract. mixture	**N-alkylated**
$MgEt_2$	Intract. mixture	Intract. mixture	**N-alkylated**	**N-alkylated**	2-alkylated
$MgPr^i_2$	**N-alkylated**	**N-alkylated**	**N-alkylated**	2-alkylated	v. slow - mixture of products

For bis(imino)pyridines containing small aryl substituents, intractable mixtures of products are produced unless bulky MgR_2 reagents are employed, while, for the least hindered metal alkyl, $MgMe_2$, an N-alkylated product is isolable only for the most hindered bis(imino)pyridine. For the combination of bulky MgR_2 with bulky bis(imino)pyridine, the N-alkylated products are destabilized in favor of products in which the alkyl group has migrated to the adjacent carbon atom within the heterocyclic ring. It is thus clear that the stability of the N-alkylated products is dependent upon a steric balance between the alkyl group and the imino aryl substituents. This delicate energetic balance is also seen to be influenced by the substituent at the imino carbon atom, since the aldimine derivative **17**, the product of the reaction between $MgPr^i_2$ and the 2,6-diisopropylphenyl aldimine ligand, is stable as the N-alkylated species. The zinc system displays closely related effects with the exception of $ZnMe_2$ which is unreactive toward bis(imino)pyridines, most probably due to the stronger Zn−C bond of $ZnMe_2$ versus ZnR_2 (R = Et, Pr, Bu, etc.) species.[10] Labeling studies on the magnesium system show that the metal-to-nitrogen migration is reversible, but only for the most hindered bis(imino)pyridine does dissociation of MgR_2 occur. The alkylation reaction is irreversible (or at least exceedingly slow) in the case of alkylzinc reagents. However, if the zinc alkyl group of an N-alkylated species is first abstracted by a strong Lewis acid, the N-attached alkyl group does then migrate to the zinc center.

Mechanism. The experimental observations indicate that the first step of the reaction involves coordination of the metal alkyl by the ligand to give a simple adduct (Scheme 13). Crossover

Scheme 13

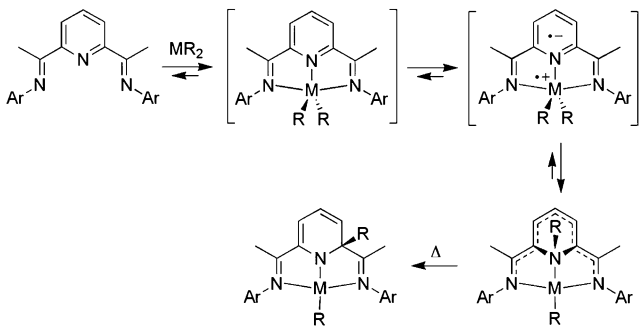

experiments have shown that complexation is reversible for DIPP derivatives but irreversible for the sterically less hindered DMP systems. Terdentate complexation of the bis(imino)-

pyridine directs the alkylation away from the imino functionality, which would at first appear to be the most likely site of alkylation. Furthermore, attack at the imino carbon or nitrogen atoms is disfavored by the presence of the ortho substituents attached to the aryl groups. Once coordinated by the ligand, it seems that the only site that can be alkylated directly is the pyridine nitrogen which leads to a reduction in the steric crowding around the metal center in the pentacoordinated precursor. The EPR experiments on the magnesium system strongly implicate single electron transfer (SET) processes, the first step involving one-electron reduction of the bis(imino)-pyridine to give a radical anion. Migration of one of the magnesium alkyl groups then affords the diamagnetic N-alkylated species. Although the loss of aromaticity of the pyridine ring is unfavorable, this is partially compensated by the extensive delocalization of the negative charge between the imine nitrogens through the backbone of the ligand.

For the most sterically crowded N-alkylated complexes (such as **11**), the N-alkyl group migrates to the 2-position in what is thought to be an irreversible rearrangement to relieve the steric congestion. Although the 2-alkylated products are sterically favored, they are probably disfavored in terms of π-bonding, since they have lost both the aromaticity of the pyridine ring and the compensatory delocalization of the formal negative charge over the backbone of the ligand.

4. Conclusions

The nonelectrophilic pyridine N-alkylation reactions documented in this study are, to our knowledge, unprecedented in the long history of pyridine reaction chemistry.[12] That such transformations are seen in this system is undoubtedly attributable to the special electronic and steric characteristics of 2,6-bis(imino)pyridines. These facilitate strong binding of the bis(imino)pyridine to the main group metal centers while disfavoring attack at the imino nitrogen or carbon centers due to the presence of bulky imino aryl substituents. A further important factor is the capacity of pyridine and imino functionalities to engage in metal-to-ligand charge transfer and, under certain circumstances, even to formally accept one or more electrons. When combined with the extensive charge delocalization made possible through the two adjoining imino groups, the aromatic stabilization of the pyridine moiety is overcome. These results serve to highlight in a unique fashion the "noninnocent" behavior of the bis(imino)pyridine ligand system and may illuminate why the combination of pyridine and imino donors is so special in the metal-based chemistry and catalysis they support.

5. Experimental Details

Details for the synthesis of compounds, their characterizing data, and their reactions are collected in the Supporting Information.

X-ray Structure Determinations. Data for **7**, **8**, **11**, and **12a** were collected on a Nonius KappaCCD diffractometer with graphite monochromated Mo Kα radiation ($\lambda = 0.710\,73$ Å). In each case a single crystal coated in oil was mounted on a glass fiber in a stream of cold nitrogen gas. Unit cell parameters were refined using the whole data set. All frames of data were processed using the DENZO-SCALEPACK programs.[13] Empirical absorption corrections were applied.[14] Structure solution and refinement were carried out using SHELXL-97[15] as included in the WinGX package.[16] For **7** the diffraction was weak and limited in extent. Structure solution was by direct methods, and least squares refinement was on all F^2. Hydrogen atoms were included in riding mode. For **7** there were two independent molecules, in one of which there is disorder of the ethyl groups. For **8** there is disorder of the C(30) and C(31) methyl groups, and the lower occupancy sites were left isotropic and C−C(methyl) bond lengths in this group were restrained. Data for **18** were collected on a Bruker P4/RA diffractometer with graphite monochromated Cu Kα radiation ($\lambda = 1.54\,178$ Å) using the low-temperature oil drop technique. Structure solution and refinement were carried out using the SHELXTL program system.[17] Hydrogen atoms were included in riding mode.

Acknowledgment. The Engineering and Physical Sciences Research Council, UK, is thanked for a studentship to I.J.B. Dr. D. Oduwole (Queen Mary and Westfield College, London, UK) and Drs. E. McInnes and J. Wolowska (University of Manchester, UK) are thanked for assistance with EPR measurements and simulations.

Supporting Information Available: Experimental procedures and characterization data, crystallographic data for structures **7**, **8**, **11**, **12a**, and **18**. This material is available free of charge via the Internet at http://pubs.acs.org.

JA042657G

(12) For a detailed review, see: Scriven, E. F. V. In *Comprehensive Heterocyclic Chemistry*; Katritzky, A. R., Rees, C. W., Boulton, A. J., McKillop, A., Eds.; Pergamon Press: Oxford, 1984; Vol. 2, p 165.

(13) Otwinowski, Z.; Minor, W. In *Processing of X-ray Diffraction Data Collected in Oscillation Mode*; Carter C. W., Jr., Sweet, R. M., Eds.; Methods in Enzymology, Vol. 276: Macromolecular Crystallography, Part A; Academic Press, 1997; pp 307−326.
(14) Blessing, R. H. *Acta Crystallogr., Sect. A* **1995**, *51*, 33.
(15) Sheldrick, G. M. *SHELX97: Programs for Crystal Structure Analysis*, release 97-2; Institüt für Anorganische Chemie der Universität: Tammanstrasse 4, D-3400 Göttingen, Germany, 1998.
(16) Farrugia, L. J. L. *Appl. Crystallogr.* **1999**, *32*, 837.
(17) *SHELXTL PC*, version 5.03; Siemens Analytical X-ray Instruments, Inc.: Madison, WI, 1994. *SHELXTL PC*, version 5.1; Bruker AXS: Madison, WI, 1997.